Available online at www.sciencedirect.com
ScienceDirect
Biochimica et Biophysica Acta 1768 (2007) 90–99
Biochimica et Biophysica Acta BBA
www.elsevier.com/locate/bbamem

Atomic force microscope visualization of lipid bilayer degradation due to action of phospholipase A_2 and *Humicola lanuginosa* lipase

Konstantin Balashev [a,b,d,*], N. John DiNardo [b,c], Thomas H. Callisen [c], Allan Svendsen [c], Thomas Bjørnholm [d]

[a] *Sofia University, Department of Physical Chemistry, Lab. Of Biophysical Chemistry, Sofia 1164, 1, James Bourchier Ave., Bulgaria*
[b] *Drexel University, Physics Department, Philadelphia, PA 19104, USA*
[c] *Novozymes, Smørmosevej 25, DK-2880 Bagsværd, Denmark*
[d] *Nano-Science Center, Department of Chemistry, University of Copenhagen, Universitetsparken 5, 2100 Copenhagen Ø, Denmark*

Received 27 April 2006; received in revised form 25 September 2006; accepted 26 September 2006
Available online 6 October 2006

Abstract

An important application of liquid cell Atomic Force Microscopy (AFM) is the study of enzyme structure and behaviour in organized molecular media that mimic in-vivo systems. In this study we demonstrate the use of AFM as a tool to study the kinetics of lipolytic enzyme reactions occurring at the surface of a supported lipid bilayer. In particular, the time course of the degradation of lipid bilayers by Phospholipase A_2 (PLA_2) and *Humicola Lanuginosa* Lipase (HLL) has been investigated. Contact mode imaging allows visualization of enzyme activity on the substrate with high lateral resolution. Lipid bilayers were prepared by the Langmuir–Blodgett technique and transferred to an AFM liquid cell. Following injection of the enzyme into the liquid cell, a sequence of images was acquired at regular time intervals to allow the identification of substrate structure, preferred sites of enzyme activation, and enzyme reaction rates.

Keywords: Atomic force microscopy; Phospholipase A_2; Humicola lanuginose lipase; Supported bilayer; Enzyme kinetics

1. Introduction

The invention of the first scanning tunneling microscope by Binnig et al. [1] paved the way for the development of a family of related techniques, commonly known as scanning probe microscopies, which includes Atomic Force Microscopy (AFM). A decisive step for the application of AFM to the study of biological samples was made by Prater et al. [2] who demonstrated that imaging biological surfaces in buffer solutions was possible. The development of commercial AFMs to allow operation in liquid environments has since led to burgeoning research on biological systems with nanometre scale resolution [3]. The capability of AFM "to look" directly at biomaterials on surfaces or at the surfaces of biomaterials themselves, coupled with the fact that virtually all living systems interact via surfaces (e.g., membrane surfaces), makes AFM a most promising technique in surface biology.

Particularly attractive areas of biological AFM applications are the study of enzyme structure and enzyme behaviour in organized molecular media that mimics in-vivo systems [4]. The first direct observation of single enzyme activity was demonstrated by Radmacher et al. [5], revealing the potential of AFM as an instrument for studying the dynamics and evolution of enzymatic processes. Direct visual evidence of supported bilayer hydrolysis by Phospholipase A_2 (PLA_2) was presented by Grandbois et al. [6]. Neilsen et al. showed lag-burst kinetics with AFM and related the phenomenon to the bilayer nanostructure [7,8]. Recently, Balashev et al. [9] demonstrated that AFM can be applied as an analytical instrument to the study of the kinetics of enzyme reactions. Several series of images obtained during hydrolysis of supported lipid layers were analyzed as a function of enzyme concentration. Using the fact that defects in the lipid lattice

* Corresponding author. Sofia University, Department of Physical chemistry, Lab. Of Biophysical Chemistry, Sofia 1164, 1, James Bourchier Ave., Bulgaria. Fax: +359 2 9625438.
E-mail address: fhkb@chem.uni-sofia.bg (K. Balashev).

0005-2736/$ - see front matter © 2006 Elsevier B.V. All rights reserved.
doi:10.1016/j.bbamem.2006.09.028

structure of a gel-phase membrane may act as initiation points for enzyme activity, Clausen-Schaumann et al. [10] combined a biological implement (enzyme reaction) with nanotechnology (AFM) and developed an enzyme-assisted lithographic technique that is applicable for local hydrolysis of a supported membrane.

Lipases and phospholipases are enzymes that have received considerable attention [11]. Phospholipases are involved in different metabolic pathways that play key roles in membrane turnover and signal transduction. Lipases have diverse physiological functions in food and fat degradation, and they are used in many biotechnological applications as well [12,13].

Phospholipase A_2 (PLA_2) is a water-soluble enzyme which is interfacially activated, and its activity strongly depends on the morphology and physico-chemical characteristics of the substrate [14]. Several methods have been employed for monitoring the surface activity of the enzyme. For example, monolayer studies at the air–water interface [15], electrochemical methods [16], fluorescence spectroscopy [17], and fluorescence microscopy [18] have been applied. The kinetics of PLA_2 hydrolysis of bilayer substrates under certain conditions demonstrates so called lag-burst behaviour, where the rate of hydrolysis rapidly changes from low to high values [19]. The duration of the lag phase depends on a number of properties of the bilayer and particularly on the existence and accumulation of products in the bilayer. The degree of compositional heterogeneity and the number of bilayer defects have been correlated to the duration of the lag time [8].

Lipases (triglyceride hydrolases) are a group of structurally well-characterized, interfacially active enzymes [20,21]. The study of enzyme reaction kinetics in organized substrate media, however, still faces difficulties because triglycerides have very weak amphiphilic character. Triglycerides are virtually insoluble in water and either adsorb on the available surface or form droplets. Their inability to be organized in well-defined substrates with measurable surface area makes it extremely difficult to obtain exchange rates between coexisting surfaces [22].

Interfacial lipolytic catalysis on monolayers was established by Verger and deHaas [23] and developed systematically by two groups—Verger et al. [11,15] and Brockman et al. [24,25]. The monolayer technique has proven to be the most reliable method for interfacial kinetics studies. The method has many advantages but one is indisputable—control over interfacial quality of the surface. This allows molecular orientation, conformational state, packing density, molecular dipole moment, and lateral viscosity to be controlled by means of surface pressure and monolayer composition. Even given the uniqueness of the monolayer technique for studying enzyme reactions occurring at the air–water interface, it has limited abilities for studying the enzyme–substrate interactions and fine monolayer structure (e.g., monolayer heterogeneity).

Fluorescence microscopy has proven to be a well-suited complementary technique in this respect [18]. Using this method, the existence of solid analogous lipid domains in the phospholipid monolayers, which PLA_2 can recognize and hydrolyze, has been shown [18]. Fluorescence microscopy only brings space resolution to the micrometer scale, however. Applying time series AFM for imaging the process of degradation of supported phospholipid bilayers greatly improves the spatial resolution to ~10 nm such that enzyme behaviour on a gel phase membrane can be analyzed [6].

Another interesting issue regarding hydrolysis of a bilayer is the synergetic (simultaneous) action of different lipases and phospholipases on mixed lipid/phospholipid substrates. It has been reported by Verger et al., [26] that when a mixed glyceride/phospholipid emulsion (Intralipid ™) is used as a substrate, PLA_2 or gastric lipase alone cannot typically degrade the glyceride molecules. However, after partial lipolysis of the monomolecular film by gastric lipase, the catalytic action of pancreatic lipase can commence immediately. It was concluded that the delay of hydrolysis is a result of lower penetration ability of pancreatic lipase.

The present study has two purposes. First, we report time-series imaging of the degradation process of supported mixed Dipalmitoylphosphocholine/Dipalmitoylglycerol (DPPC/DPG) double-layers due to enzyme action of PLA_2. The phospholipid/lipid mixtures were chosen to overcome the inability of the lipid to generate well-defined bilayer structures. In this way it was possible to obtain stable bilayers and stable imaging with AFM. Second, bilayers were used as a substrate for simultaneous action of HLL and PLA_2 to allow the study of the synergetic action of two enzymes.

2. Materials and methods

2.1. Lipids

1,2-Dipalmitoyl-*sn*-glycero-3-phosphocholine (DPPC) and 1,2-Dipalmitoyl-*sn*-glycerol (DPG) were purchased from Avanti Polar Lipids (Alabaster, AL) and Sigma (St. Louis, MO), respectively. Both lipid samples were used as received. Other chemicals and salts were purchased from Merck (Germany) or Sigma. A HEPES buffer (10 mM HEPES (pH 8.0), 150 mM KCl, 30 μM $CaCl_2$, and 10 μM EDTA) was used to prevent extensive calcium-palmitate precipitation and minimize concentration changes of the co-factor Ca^{2+} at the bilayer surface upon formation of negatively-charged fatty acids.

2.2. Enzymes

Snake venom PLA_2 from *Agkistrondon piscivorus* (Sigma, St. Louis, MO) was used. We used a HEPES buffer (10 mM HEPES, 150 mM KCl, 30 μM $CaCl_2$, and 10 μM EDTA, pH 8.0), which prevents extensive calcium palmitate precipitation and minimizes changes in the Ca^{2+} concentration at the bilayer surface when negatively charged fatty acid molecules are present. The enzyme concentration was 100 nM.

Humicola lanuginose lipase (HLL) was provided by Novozymes A/S and diluted with the same HEPES buffer to concentrations of 600 nM.

2.3. Bilayer preparation

Mixed monolayers of DPPC and DPG were prepared on a commercial Langmuir trough (KSV 5000, KSV, Helsinki, Finland). Freshly cleaved mica was used as the solid support, having been immersed in the subphase before the spreading of the lipids. Initially, DPPC and DPG were dissolved in chloroform to a concentration of 1 mg/ml. From these stock solutions, mixtures of DPPC/DPG (initial concentrations of 70:30, mol/mol) were produced. The lipids were spread on a pure MilliQ (Millipore Corp., Bedford, MA) water surface, and 15–30 min was allowed for solvent evaporation. The monolayers were compressed at a constant speed of 1 $Å^2$/molecule/min to a final surface pressure in the liquid-condensed phase of typically 30–35 mN/m. We obtained isotherms for

DPPC and DPG individually, and also for their mixture; these isotherms are similar to those previously reported [27]. We chose to work with a Ca^{2+}-free subphase to avoid creating micron-sized domains characteristic of large-scale phase separation in the monolayers [27]. Without calcium, we were able to create a bilayer that resembles vesicular systems and that were more closely related to a bilayer that has been partially degraded by the enzyme [7]. As a solid supports for LB transferring were used mica discs Grade V-4 Muscovite with diameter of 12 mm (Structure Probe Inc./SPI Supplies, West Chester, PA). Lipid layers were transferred vertically onto the mica supports at 1 mm/min, with a 15 min wait between the first and second layer. Only double layers with transfer ratios close to 1 were used (Fig. 1A). Supported bilayers with an initial concentration of DPPC 70% and DPG 30% were prepared. The supported bilayers were kept under water and immediately transferred to the fluid cell of the AFM.

2.4. AFM imaging

A Nanoscope IIIa system (Digital Instruments, Santa Barbara, CA) equipped with a fluid cell was used for all imaging. A standard silicon O-ring was used to seal the fluid cell. The cell was flushed with HEPES buffer without enzyme before imaging. Cantilevers with oxide-sharpened silicon nitride tips (NanoProbes, Santa Barbara, CA) with a nominal spring constant of 0.06 N/m were used for scanning. The bilayer was equilibrated in the fluid cell for at least 30 min to reduce cantilever drift before enzyme injection. All imaging was carried out in contact mode with a loading force of less than 500 pN, and the force was maintained at a minimum by manual adjustment of the set point. The scan rates were between 2 and 4 Hz (i.e., 4.2–2.1 min/image). To minimize any influence of the tip on hydrolysis, every other frame was scanned with the tip away from the surface except at the very beginning of hydrolysis. Under these conditions, the bilayer can be imaged repeatedly [28,29], even during hydrolysis [6,7]. As an additional control in all experiments described here, the scan area was increased and/or moved after each experiment to check that hydrolysis had taken place over the entire sample. We found that the extra area/areas scanned were similar to the area analyzed, confirming hydrolysis across the sample. All images were plane fit to remove sample tilt. Fig. 1B schematically illustrates the situation in the fluid cell during enzyme hydrolysis of the bilayer. Note particularly the distinct height difference between the top of the bilayer and bilayer-deep holes.

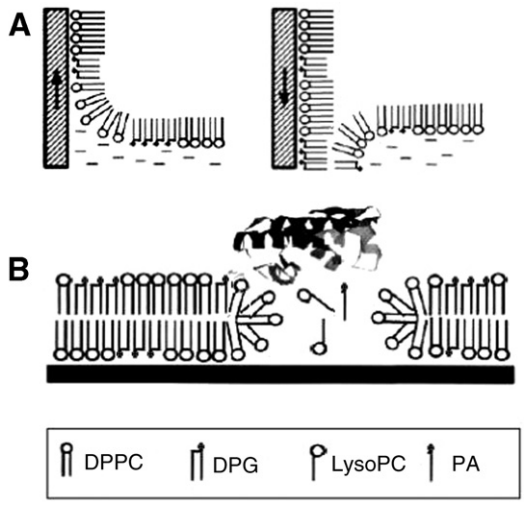

Fig. 1. (A) Schematic illustration of the transfer of the mixed monolayers to a solid support. First a monolayer of DPPC and DPG was transferred to the solid support (mica), and then a double layer was formed after dipping down the support. (B) In the AFM, the bilayer was hydrolyzed by the enzyme (shown schematically as phospholipase A2 crystal structure), which created additional product molecules (LysoPC and palmitic acid (PA) for example are as a result of PLA_2 action). The structure of the bilayer was observed by the AFM, especially the height difference between the top of the bilayer and the mica.

2.5. Image analysis

Image analysis was carried out using two public domain programs—Image SXM on a Macintosh computer and Scion Image, the equivalent PC program (both available on the Internet at http://rsb.info.nih.gov/nih-image). Because the AFM scans took between 2.1 and 4.2 min to complete, it was necessary to divide the AFM images into "time zones". Therefore, each structural defect was assigned an individual point of time (e.g., a defect in the top of a scan could be assigned $t=1.0$ min, while another defect at the bottom of the same scan could be assigned $t=3.1$ min for a 4 Hz scan).

3. Results

In this study, AFM is used to quantify the structural changes occurring at supported mixed DPPC/DPG bilayers undergoing enzyme action. The two components of the bilayer are substrates for PLA_2 and HLL, respectively. In order to distinguish enzyme action on DPPC or on DPG molecules, we carried out three sets of experiments. The first set involved only PLA_2 present in the bulk phase. In this case only DPPC molecules embedded in the double layer were targets for enzyme attack. In the second set, only HLL was introduced into the liquid cell. For these experiments, only DPG molecules in the bilayer were expected to be hydrolyzed by the enzyme. In the third set, both enzymes were present in solution.

3.1. Experiments with PLA_2 and mixed DPPC-DPG double layers

Supported lipid membranes in the gel phase are stable upon imaging with the AFM [6]. The prepared bilayers were all imaged using an AFM liquid cell. After sample preparation of supported double layers, height differences observed in a bilayer were a result of incomplete coverage of the mica support resulting in defects appearing as holes in the bilayer. In a control experiment, one of the DPPC/DPG bilayers was imaged in the AFM liquid cell for 2 h prior to an experiment as a check for stability and tip-sample interaction effects. The bilayer was found to be stable during this period. After thermal equilibration of the liquid cell for a minimum of 30 min, the enzyme was injected into the cell and the changes in the structure of the lipid bilayer due to enzyme-induced degradation were followed over time.

Fig. 2A shows a LB film of mixed DPPC/DPG transferred onto mica in which the phospholipids are organized in a gel-phase unilamellar bilayer (see Materials and methods for details). The majority of the area (95–100%) of all freshly prepared bilayers imaged consisted of a uniform, flat bilayer with a composition corresponding to the structure of monolayers deposited from the Langmuir trough. In addition to the regular bilayer structure, holes in the membrane where the mica was not covered with molecules were observed to be a single bilayer deep. We used these defects as an indicator for the degree of hydrolysis upon enzyme injection. The height differences between the DPPC/DPG film (bright domains) and the mica (dark domains) were 4.8 ± 0.5 nm (see inset in Fig. 2B). This value is in good agreement with X-ray data for the thickness of the DPPC/DPG monolayer which is ~2.4 nm [30]. For the

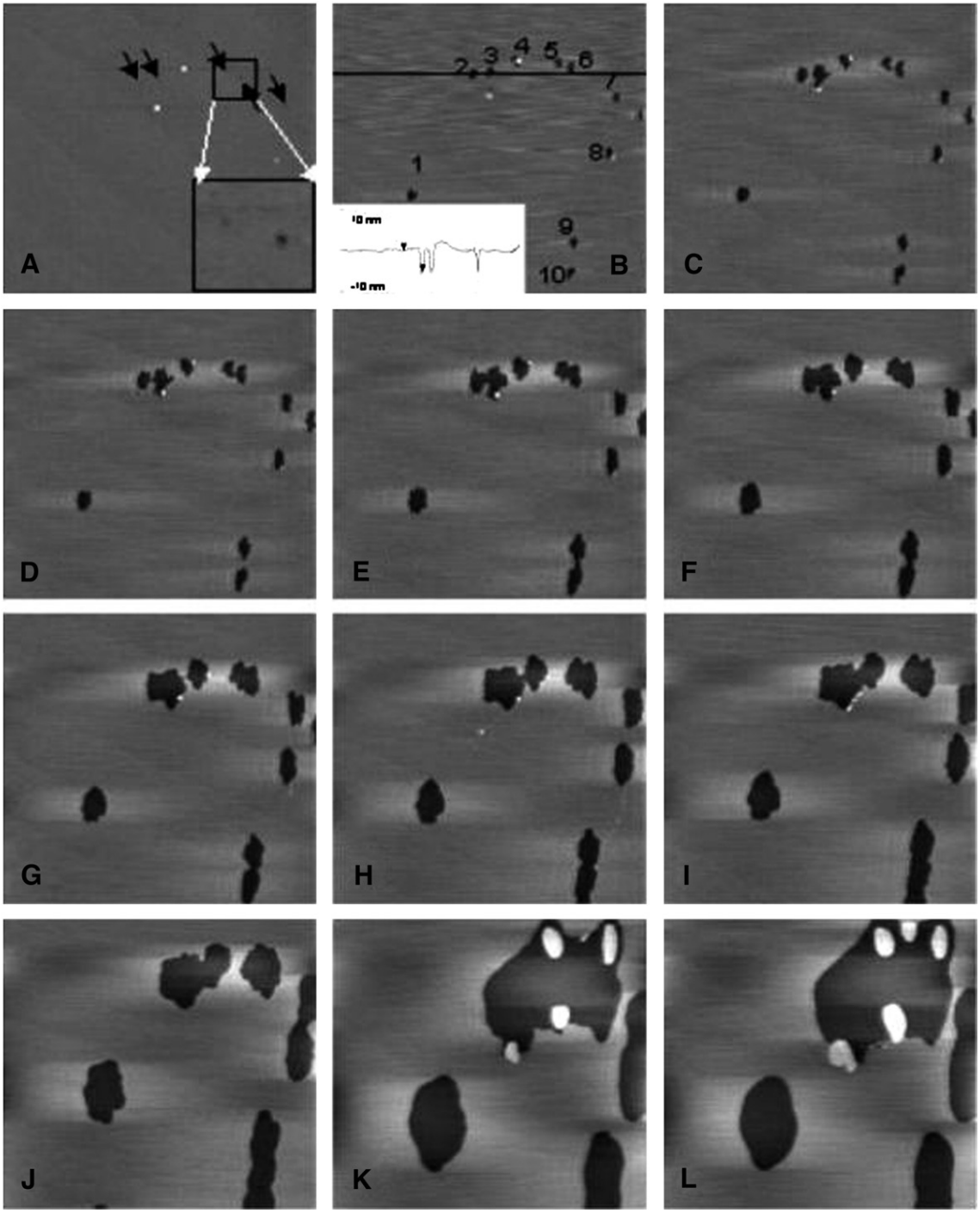

Fig. 2. Time sequence of AFM images from experiment in which 20 nM PLA_2 solution was injected into the liquid cell (scan size = 20 × 20 μm^2). Image (A) is prior to enzyme injection and the black arrows show existing initial defects (depressions) in the double layer, insertion shows a zoom in and close-ups of two of these depressions. (B) is 4 min after enzyme injection and the growing defects are numbered, and the insertion is a section analysis plot made in the marked with a line zone. (C–L) are selected images taken in the time interval 8–120 min after enzyme injection. The darker areas represent structural defects in the lipid bilayer. After enzyme injection, the initial structural defect expands as the top lipid layer is hydrolyzed and the bottom layer spontaneously desorbs.

10×10 μm^2 scanning area shown, structural defects were present in almost all the studied samples before enzyme injection. Only in 2–3 cases were we able to obtain a bilayer over this area without defects. The number of defects varied between samples, and this is presumably a result of the transfer process and sample handling. However, for all the studied samples, the area fraction covered by this type of defect was below 5%.

In Fig. 2, a typical series of images from a PLA_2 experiment is shown. The first image (A) was obtained prior to PLA_2 injection. Images B–L reveal consecutive changes due to enzyme action, with a clear increase of defect size observed just ~4 min after enzyme addition to the liquid cell (Fig. 2B). The growth of the existing holes was calculated by analysis of the AFM images. With enzyme present, holes are expected to grow

as a result of hydrolysis of the lipid molecules. The product molecules do not remain in the bilayer but desorb from the support, thus enlarging the existing holes. Determining the area fraction of holes in the membrane as a function of time gives a measure of the degree of hydrolysis at various stages. Measured this way, we assert that the degree of hydrolysis was influenced by desorption of non-hydrolyzed lipid molecules.

There are two important issues about PLA_2 action that should be noted. First, PLA_2 has been confirmed to preferably hydrolyze areas in the bilayer where product accumulation has created phase segregation in the membrane [8] or at the border of the membrane, where the phospholipids are not well packed (Fig. 1B). This is assumed to occur as a result of both the high curvature and loose molecular organization at the edge of a bilayer defect. Such molecular organization gives the best conditions for enzyme penetration, activation and catalytic activity. Second, the hydrolysis of phospholipids by phospholipase A_2 (PLA_2) has been shown to be characterized by a latency period, i.e., a period of low activity, followed by a burst [19]. The course of the reaction is determined primarily by the properties of the membrane with which the PLA_2 interacts. Special attention has been given to the duration of the latency period, which can be modulated by altering the experimentally accessible parameters such as Ca^{2+} concentration, ionic strength, temperature, lipid composition, etc. [19].

Analysis of the AFM images in Fig. 2 shows that hydrolysis of the mixed DPPC/DPG bilayer is initiated at certain membrane locations where either traces of structural double layer defects (holes) are identified or some small depressions in the double layer have been observed (see arrows in Fig. 2A and a close up of the depression in the inset). It is evident that hydrolysis of the bilayer has started in the first minutes, after injection of PLA_2 and without any lag phase activity (Fig. 2B). The existing structural defects have enlarged their size and new holes have appeared. We assume that these new defects have emerged at the membrane surface where DPPC/DPG phase segregation has occurred. It is well established that phase segregation accommodates the adsorption and activation of PLA_2 because the enzyme molecule has a preference to cluster underneath the fatty-acid-enriched domains [18,32]. Thus, our observation supports the assertion that most susceptible places for enzyme interactions are the rim of the structural defects [6,10] and the boundaries of coexisting DPPC/DPG phases [7]. The low fraction of DPG and the resolution of the obtained images allow us to monitor only traces of separate domains or phases. We believe that these domains are similar to those observed in our previous studies of mixed DPPC/Palmitic Acid (PA) double layers [31]. Because PA has a similar amphiphilic structure as DPG, the assumption of DPPC/DPG phase segregation is plausible.

A quantitative analysis of all holes in the AFM images was performed spanning the time interval of 120 min after enzyme injection to determine the change of the desorbed area (ΔA) as a function of time (Δt). At least five repeats of the experiment were performed to establish reproducibility. Fig. 3 represents a typical result of the kinetics analysis of the growing holes. In Fig. 2B, all the locations in the membrane where structural

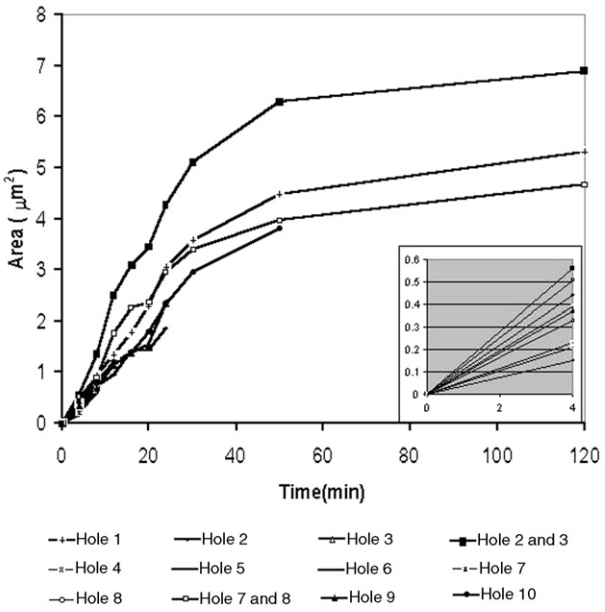

Fig. 3. Desorbed lipid areas versus time after injection of PLA_2 with concentration 100 nM. Curves show the desorbed area of the structural defects numbered at Fig. 2B with numbers 1 to 10. The inset shows the initial slope of the curves.

defects occurred after PLA_2 insertion are numbered. In all experiments, the number of holes created after PLA_2 addition remained the same. This allows us to conclude that, once the enzyme binds to the membrane, it is activated and starts "scooting" trough the membrane. The "scooting mode" of PLA_2 action was confirmed to be most realistic [33]. From the graphs in Fig. 3 it can be seen that the hydrolyzed area of all structural defects grows linearly in the first 20–25 min and then levels off to an equilibrium. The different initial slopes (see inset in Fig. 3) indicate that different numbers of enzymes are acting in the scope of one defect. A challenging problem is to determine the number of active enzymes needed to establish the surface enzyme kinetics scheme. As an attempt to determine this, Yapoudjian et al. [34] adapted fluorescence resonance energy transfer technique (FRET) to study the process in which lipase is adsorbed to monomolecular lipid films spread at the air–water interface. In earlier studies, Verger et al. [35] suggested that only 1% of the enzyme molecules in the bulk phase are activated and take place in the catalytic act. Using AFM, Grandbois et al. [6] and later Risbo et al. [7] were able to achieve a resolution that allowed channel patterns in the membrane to be observed. Assuming that channel formation is a result of single enzyme action we have re-analyzed the Grandbois et al. [6] data. Numbering the channels occurring after injection of PLA_2, we calculate that only about 5% of the available for enzyme attachment perimeter length was covered by enzymes. In this calculation, we measured the initial perimeter of the existing structural defects from Fig. 2 of ref. [6] and assumed a cross-sectional diameter of 5 nm for the PLA_2 [23]. For example, one of the defects in Fig. 2 of ref. [6] was measured to have an initial perimeter length 1.452 μm and could accommodate about 290 enzymes if the PLA_2 molecules

are sitting at the edge in a shoulder-to shoulder fashion. Instead, only 13 channels appeared. Assuming that one enzyme occupies 5 nm, 13 enzymes will occupy 0.065 μm, therefore the occupancy of the perimeter is about 5%.

Furthermore, for HLL action on hybrid Monooleoylglycerol MOG/DPPC layers [9] we have determined that the occupancy of the perimeter of the existing structural defects by lipase molecules varied depending on the bulk enzyme concentration. The values of 0.3% for very dilute HLL concentrations of 2.5 nM, and between 7 and 20% for enzyme concentrations of 15–45 nM were obtained.

To analyze the initial rate of hydrolysis, the structural defects in the double layer were numbered (Fig. 2A). The hydrolyzed area versus time for each observed defect is shown in Fig. 3. Because these defects appeared immediately and without lag phase in areas without detectable structural defects and were growing at different rates, we conclude that a different number of enzymes per hole is responsible for the bilayer degradation. Assuming that only 5% of the edge of the structural defects is covered by the active enzyme molecules and that DPPC fraction of 70% should be susceptible for hydrolysis, one can estimate the number of enzymes working per hole, and on that basis the hydrolysis rate. Thus, we obtain 59±10 DPPC molecules/s/enzyme. This result correlates with 88±30 DPPC molecules/s/enzyme, reported previously [6].

Another observation regarding PLA_2 action is important—the incomplete degradation of a supported double layer. In our experiments, we observed that hydrolysis takes place at the edge of structural defects. Therefore, those structural defects present before enzyme injection expand after being exposed to PLA_2. At the same time, large areas without structural defects are surprisingly stable for the duration of the experiment. The curves in Fig. 3 show two easily distinguished regimes. There is linear growth for small times, i.e. a constant hydrolysis rate, followed by a reduction in hydrolysis rate. In fact, the rate begins decreasing ~ 25 min after enzyme addition. Consequently, none of the bilayers are completely desorbed after 2.5 h. Directly observed phenomena in the AFM experiment (Fig. 2) can be explained by the following molecular events (Fig. 4): (i) the enzymes are preferentially activated at the edge of a structural defect or at the border of coexisting phases (Fig. 4B). In a hypothesized rate-limiting step, PLA_2 hydrolyzes DPPC to LysoPC and Palmitic acid (Fig. 4C). The hydrolysis of DPPC molecules at the upper layer leads to the exposure of hydrophobic tails of bottom-layer DPPC/DPG molecules to the aqueous phase. In a kinetically fast step, unfavourably oriented DPPC molecules spontaneously desorb and most likely form lipid aggregates (vesicles, micelles, etc.), which are either dissolved in the aqueous phase (Fig. 4C) or remain as adsorbed aggregates inside the structural defects. In the end, the hydrolysis of the lipid substrate is inhibited due to binding of all free enzymes to the formed DPPC and/or DPG aggregates of either soluble vesicles (Fig. 4D) or double-layer structures formed at the solid–liquid interface (Fig. 4E). Thus, the incomplete hydrolysis suggests that the hydrolysis products and/or the desorbed DPPC/DPG molecules and their aggregates inhibit the enzyme. Most likely the inhibition is caused by the

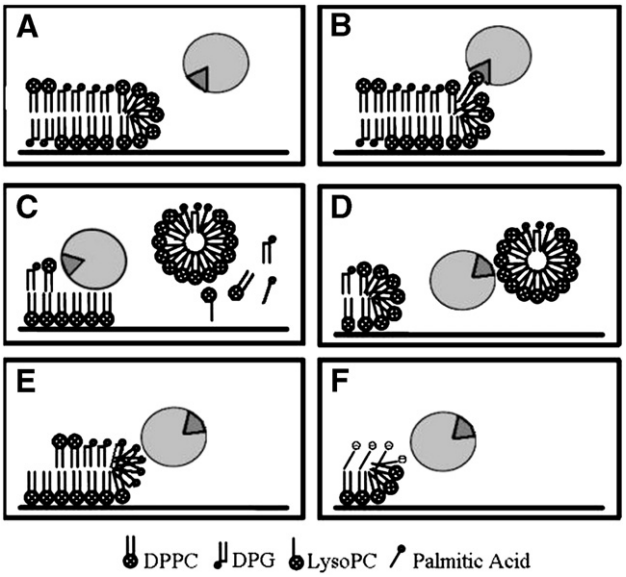

Fig. 4. Schematic illustration of the kinetic steps involved in the lipid bilayer desorption observed by AFM. (A) The enzyme adsorbs to the lipid film. (B) The enzyme is activated at the edge of structural defects. (C) Hydrolysis occurs in the hypothesized rate limiting step, and spontaneously desorbed DPPC and DPG and hydrolysis products LysoPC and Palmitic acid (PA) molecules form aggregates. Incomplete hydrolysis is likely to be caused by one or more of the following events: (D) Binding of PLA_2 to the aggregates either to soluble aggregates. (E) Binding to aggregates formed at the solid surface. (F) Changes in the physico-chemical properties of the interface due to fatty acid hydrolysis products remaining in the lipid film.

extremely low Critical Micelle Concentration (CMC) of DPPC (5×10^{-10} M) [9], which causes all desorbed DPPC and DPG molecules to form aggregates of micelles, vesicles, etc. In the experimental data shown in Fig. 2B, the desorbed area of DPPC and DPG in the first scan after PLA_2 addition, is 2.57 μm^2. For a DPPC fraction of 70%, the number of DPPC molecules occupied that area is 4×10^6 ($0.7\times$desorbed area/MMA_{DPPC}). Introducing the term "scan area volume", defined as the volume of buffer divided by the scan area, the concentration of DPPC can be estimated. Using a scan area volume of 5×10^{-11} dm^3 (Scan area: 1×10^2 μm^2, height of the liquid cell: 0.5 mm) the formal concentration of DPPC is 1.3×10^{-7} M after 4 min. This DPPC concentration is several hundred times the CMC. The aggregates formed as a consequence of exceeding the CMC are ideal for binding free enzymes [14,30]. Thus, hydrolysis is most likely halted as a result of PLA_2 binding to the DPPC or/and DPG aggregates.

3.2. Experiments with HLL and mixed DPPC-DPG double layers

In contrast to the previous experiments, injection of HLL into the liquid cell does not result in any detectable changes in double layer structure. A typical example is given in Fig. 5. Initially some small aggregates with sizes between 0.1 and 0.5 μm (see arrows in Fig. 5A) were noticed before the enzyme injection. After 3.5 h these aggregates completely disappeared. Their molecular nature is unknown. It could be assumed that

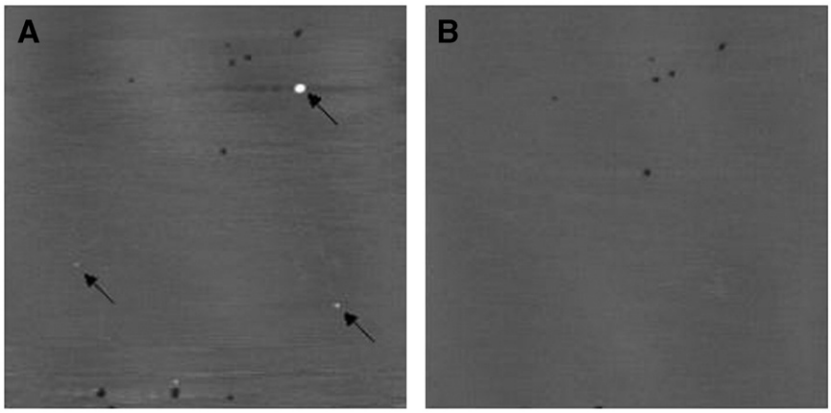

Fig. 5. AFM images from experiment where a 200 nM HLL solution was injected into the liquid cell (scan size 20 × 20 μm^2). Image (A) is prior to enzyme injection and (B) is 210 min after enzyme injection. No visible changes in double layer structure were detected. Initially some spots (see arrows at A) with sizes between 0.1 and 0.5 μm before enzyme injection were noticed then after they gradually disappeared. The nature of these particles is unknown; they are either some excess lipid aggregates or some salt crystals.

they are either some excess lipid aggregates or some salt crystals that have been eventually dissolved in the bulk phase. If these were lipid aggregates, it is not clear if they were dissolved as a result of lipase action.

In all of our experiments, we observed no visible changes in the bilayer. It remained intact and stable, indicating lack of HLL activity. Such an observation is not unexpected, though. Phospholipids are considered to be lipase inhibitors [35]. Brockman H.L. [36] has shown, that, for pancreatic lipases below 0.4 mol fraction of diacylglycerol and absence of co-lipase, less then 10% hydrolysis occurred. This result is explained as due to poor accessibility of the substrate molecules. However, when the mol fraction increased between 0.4 and 0.6 mol fraction then hydrolysis also increased substantially. An almost identical observation was reported for pancreatic carboxyl ester lipase [37]. On the basis of these findings, a model for the initiation of lipolysis at the phosphatidylcholine-rich surface was suggested [37]. Accordingly, small lipid fractions correspond to a small number of sites at the interface where the enzyme can be adsorbed. Additionally, even if attached, the enzyme has a limited amount of substrate molecules available for hydrolysis. Although clear evidence was not presented, the possible explanations could be restricted lateral diffusion of the substrate molecules or the inactive (open) conformation of the enzyme at the interface [37].

As noted above, we can assume that the lack of activity of HLL on mixed DPPC/DPG (0.7 mol/0.3 mol) is a result of the low mol fraction of DPG. We were not able to perform experiments with higher than 0.3 mol DPG fractions because bilayers obtained were unstable and easily damaged after their transfer to mica support.

3.3. Experiments with PLA_2, HLL and mixed DPPC-DPG double layers

After incubating the mixed phospholipid-lipid bilayer with HLL for about 2 h and observing no structural changes, the liquid cell was flushed with a solution of PLA_2. The injected PLA_2 is not expected to flush away the HLL molecules that are firmly adsorbed on the double layer, but only these that are in the bulk phase of the liquid phase and those that are loosely attached to the bilayer surface.

Fig. 6 shows a series of images for a typical experiment. The first image (Fig. 6A) is prior to PLA_2 injection and with HLL present in the liquid cell. Only one structural defect in the double layer was observed. Images B–L show consecutive changes as a result of enzyme action. It is apparent that the desorbed area increased gradually in time. Again, the enzyme attacked only the location of the bilayer where an imperfection of the bilayer structure is observed (see arrow in Fig. 6A). It is also observed that the growing defect had a finger-like shape with a more profoundly developed channel-like pattern. That pattern was similar to one observed in the action of PLA_2 on DPPC bilayers [6]. In the inset of Fig. 6C, we hypothesize that the darkened areas of the hole are degraded by single enzymes. Assuming that about 5% of the edge of the structural defect can accommodate enzyme molecules and, taking into account the fact that the perimeter length of the initial defect is 0.69 μm, it is found that the expected number of enzymes (~9) and the number of finger-like protrusions (artificially darkened regions in Fig. 6C) are similar.

In Fig. 7, we compare the kinetics from the PLA_2-only experiment (curve B) with the experiment where both PLA_2 and HLL are present (curve A). Fig. 7 (curve A) shows enzyme kinetics obtained from the image sequence of Fig. 6 in which only one defect is present. It is apparent that the lag-burst phenomenon is absent and after injecting PLA_2 an immediate increase of hydrolyzed area occurs. To plot curve B we first normalised the total hydrolyzed area by the number of defects, which is 10 (Fig. 2). It is more accurate to use the normalised instead of total area because of the assumptions that only the edge of the defects will accommodate enzymes and the number of these enzymes remains constant. It is apparent that when both PLA_2 and HLL are acting the kinetics curve has an "S" shape and exhibits three well-distinguished phases (see Fig. 7, curve A). We assume that the first phase of the double layer hydrolysis is a result only of PLA_2 action. The same initial rates for both

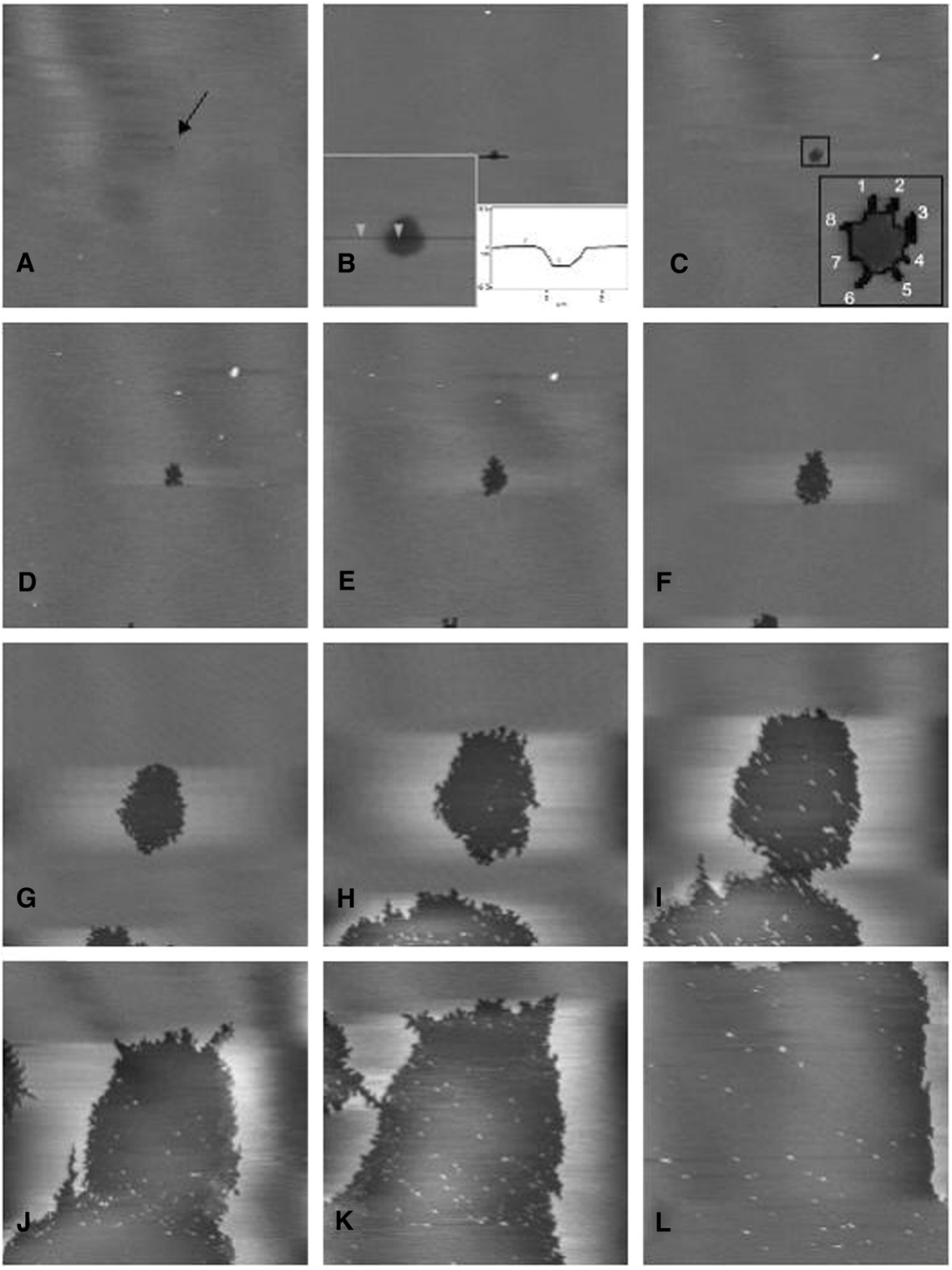

Fig. 6. Time sequence of AFM images from an experiment where both enzymes are present. First HLL was injected and incubated in the liquid cell for 2 h. Then PLA_2 solution was introduced into the liquid cell. Image (A) is prior to PLA_2 injection and the arrow shows existing of an initial structural defect in the double layer, (B) is 4 min after PLA_2 injection. The insets are the magnification of the growing defect and its depth respectively, (C–L) are selected images taken in the time interval 8–270 min after enzyme injection The darker areas represent structural defects in the lipid bilayer. After enzyme injection, the initial structural defect expands as the top lipid layer is hydrolyzed and the bottom layer spontaneously desorbs. Inset in C shows the magnification of the structural defect and numbers correspond to possible number of enzymes hydrolyzed the darkened area. Scan size was 20×20 μm^2.

experiments and the overlap of curves A and B (see inset in Fig. 7) in the first 25 min supports that assumption. The second phase (see arrow 1 in Fig. 7, curve A) is a burst of enzyme activity. We assume that this second burst may be triggered by the HLL activity. As the reaction of PLA_2-catalysed DPPC hydrolysis occurs, a DPPC fraction is transformed to Palmitic acid and

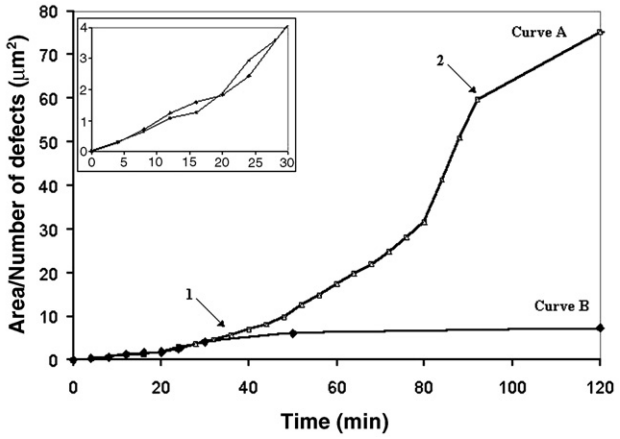

Fig. 7. Normalised by the number of defects area versus time after PLA_2 injection with or without a presence in the liquid cell of HLL. Curve A (PLA_2 and HLL) and curve B (PLA_2) show the (desorbed area/number of defects) calculated from image series at Figs. 2 and 4, respectively. The inset shows the initial slopes of the two curves. Arrows show the start of a phase in the enzyme kinetics (see text).

LysoPC. The percentage of DPPC molecules decreases and when it is sufficiently low (below 0.6 mol fraction) comparatively to DPG the HLL begins to act [36]. Another molecular-level process that favours HLL activation is PLA_2-induced compositional change in the upper monolayer (top layer of the bilayer). It is also possible that small DPG enriched domains move by lateral diffusion and merge to form larger DPG areas in the original bilayer structure. Eventually, after 1 h, the hydrolysis of the supported bilayer slows down sufficiently and the hydrolyzed surface area again reaches saturation as a result of the enzyme inhibition described in Fig. 4. To explain all molecular events occurring at the double layer surface, we can apply the same molecular scheme, adding also the lateral diffusion and merging of the DPG-domains in the bilayer structure and HLL activation and action on the bilayer.

4. Discussion

Using the LB technique, we prepared a mixed DPPC/DPG (0.7 mol/0.3 mol) bilayer as a substrate for phospholipase (PLA_2) and lipase (HLL) action. The bilayers exhibited a well-defined structure, and proved to be very suitable for both qualitative and quantitative analysis of interfacial lipolytic action. The degradation process was visualized using liquid-cell atomic force microscopy. In three separate series of experiments, we exposed the bilayers to PLA_2, HLL, and PLA_2+HLL action, respectively. In the first and the third experimental series (PLA_2 and PLA_2+HLL), we clearly observed degradation of supported bilayers. Only initial structural defects were attacked by the enzyme, confirming earlier experimental findings that PLA_2 and HLL are activated by substrates with high curvature [12,22]. In the second experimental series, injecting HLL into liquid cell did not lead to hydrolyses of supported bilayers. This lack of enzyme activity is explained as a result of the low mol fraction of DPG. We were not able to perform experiments with higher then 0.3 mol fractions DPG because the obtained bilayers were unstable and easily damaged after their transfer to a solid support. In the third series of experiments (PLA_2+HLL) the enzyme activity was triggered when the PLA_2 partially hydrolyzed the supported bilayer. After analyzing the kinetics it was determined that when the two enzymes are present in the liquid cell, PLA2 partially hydrolyses the bilayer and then the burst of activity occurs as result of HLL involvement in the catalytic act. The AFM images obtained also allowed us to determine the preferred sites of enzymatic action. Observation and analysis of the pattern of the hydrolyzed bilayer show that the edges of the structural defects in the bilayer are not saturated with enzyme molecules in shoulder to shoulder fashion. Only 5% of the available perimeter length of these defects is covered by PLA_2 molecules. Finally, we have determined an initial rate of hydrolysis of ~59 DPPC molecules/s/enzyme which correlates with previously published results using a different approach [6]. Our findings also confirmed our earlier published results describing preferred sites of activation of Phospholipase A_2 (PLA_2), which has been found to discriminate between structural and compositional defects [7].

Acknowledgements

We thank Shamkant Anant Patkar, Novozymes A/S, for purifying all HLL samples. Financial support from the European Community through the project “Lipid structure and lipases, BIO4 CT 972365”, the Danish Research Council and the PA Nanotechnology Institute are gratefully acknowledged. We thank Dr. Robert Verger for fruitful discussions. We also thank Dr. Richard DiDio of LaSalle University for critical reading of the manuscript.

References

[1] G. Binnig, C.F. Quate, C. Gerber, Atomic force microscope, Phys. Rev. Lett. 56 (1986) 930–933.
[2] C.B. Prater, H.J. Butt, P.K. Hansma, Atomic force microscopy, Nature 345 (1990) 839–840.
[3] H.G. Hansma, Surface biology of DNA by atomic force microscopy, Annu. Rev. Phys. Chem. 52 (2001) 71–92.
[4] H. Lin, D.O. Clegg, R. Lal, Imaging real-time proteolysis of single collagen I molecules with an atomic force microscope, Biochemistry-US 38 (1999) 9956–9963.
[5] M. Radmacher, M. Fritz, H.G. Hansma, P.K. Hansma, Direct observation of enzyme activity with the atomic-force microscope, Science 265 (1994) 1577–1579.
[6] M. Grandbois, H. Clausen-Schaumann, H.E. Gaub, Atomic force microscope imaging of phospholipid bilayer degradation by phospholipase A(2), Biophys. J. 74 (1998) 2398–2404.
[7] L.K. Nielsen, J. Risbo, T.H. Callisen, T. Bjørnholm, Lag-burst kinetics in phospholipase A(2) hydrolysis of DPPC bilayers visualized by atomic force microscopy, BBA-Biomembr. Acta 1420 (1998) 266–271.
[8] L.K. Nielsen, K. Balashev, T.H. Callisen, T. Bjørnholm, Influence of product phase separation on phospholipase A2 hydrolysis of supported phospholipid bilayers studied by force microscopy, Biophys. J. 83 (2002) 2617–2624.
[9] K. Balashev, M. Gudmand, L. Iversen, T.H. Callisen, A. Svendsen, T. Bjørnholm, *Humicola lanuginosa* lipase hydrolysis of mono-oleoyl-rac-glycerol at the lipid–water interface observed by atomic force microscopy, BBA-Biomembranes 1615 (2003) 93–102.
[10] H. Clausen-Schaumann, M. Grandbois, H.E. Gaub, Enzyme-assisted nanoscale lithography in lipid membranes, Adv. Mater. 10 (12) (1999) 49.

[11] R. Verger, G.H. deHaas, Interfacial enzyme-kinetics of lipolysis, Annu. Rev. Biophys. Bio. 5 (1976) 77–117.
[12] M.H. Gelb, M.K. Jain, A.M. Hanel, O.G. Berg, Interfacial enzymology of glycerolipid hydrolases: lessons from secreted phospholipases A2, Annu. Rev. Biochem. 64 (1995) 653–688.
[13] M. Waite, The Phospholipases, Plenum Press, New York, 1987.
[14] I. Panaiotov, R. Verger, in: A.W.N.W. Bazkin (Ed.), Physical Chemistry of Biological Interfaces, Marcel Dekker, New York, 2000, pp. 359–400.
[15] S. Ransac, H. Moreau, C. Riviere, R. Verger, Monolayer techniques for studying phospholipase kinetics, Method Enzymol. 197 (1991) 49–65.
[16] S. Chen, H.D. Abruna, Enzymatic activity of a Phospholipase A2: an electrochemical approach, Langmuir 13 (1997) 5969–5973.
[17] M.K. Jain, B.P. Maliwal, Spectroscopic properties of the states of pig pancreatic phospholipase A2 at interfaces and their possible molecular origin, Biochemistry-US 32 (1993) 11838–11846.
[18] D.W. Grainger, A. Reichert, H. Ringsdorf, C. Salesse, Hydrolytic action of phospholipase A2 in monolayer phase transition region: direct observation of enzyme domain formation using fluorescence microscopy, BBA-Biomembranes 1023 (1990) 365–379.
[19] R. Apitz-Castro, M.K. Jain, G.H. De Haas, Origin of the latency phase during the action of phospholipase A2 on unmodified phosphatidylcholine vesicles, BBA-Biomembranes 688 (1982) 349–356.
[20] D.M. Lawson, A.M. Brzozowski, G.G. Dodson, R.E. Hubbard, B. Huge-Jensen, E. Boel, Z.S. Derewenda, in: P. Woolley, S.B. Petersen (Eds.), Lipases; Their Structure, Biochemistry and Application, Cambridge Univ. Press, Cambridge, 1994, pp. 77–95.
[21] K. Thirstrup, R. Verger, F. Carriere, Evidence for a pancreatic lipase subfamily with new kinetic-properties, Biochemistry-US 33 (1994) 2748–2756.
[22] O.G. Berg, Y. Cajal, G.L. Butterfoss, R.L. Grey, M.A. Alsina, B.Z. Yu, M.K. Jain, Interfacial activation of triglyceride lipase from thermomyces (Humicola) lanuginosa: kinetic parameters and a basis for control of the lid, Biochemistry-US 37 (1998) 6615–6627.
[23] R. Verger, G.H. deHaas, Enzyme reactions in a membrane model: 1. New technique to study enzyme reactions in monolayers, Chem. Phys. Lipids 10 (1973) 127–136.
[24] H.L. Brockman, F.J. Kezdy, J.H. Law, Isobaric titration of reacting monolayers-kinetics of hydrolysis of glycerides by pancreatic lipase-B, J. Lipid Res. 16 (1975) 67–74.
[25] W.E. Momsen, H.L. Brockman, Recovery of monomolecular films in studies of lipolysis, Method Enzymol. 286 (1997) 292–305.
[26] Y. Gargouri, H. Moreau, R. Verger, Gastric lipases: biochemical and physiological studies, BBA-Lipid Lipid Met. 1006 (3) (1989) 255–271.
[27] K.M. Maloney, D.W. Grainger, Phase separated anionic domains in ternary mixed lipid monolayers at the air–water interface, Chem. Phys. Lipids 65 (1993) 31–42.
[28] Z. Shao, J. Yang, Progress in high resolution atomic force microscopy in biology, Q. Rev. Biophys. 28 (1995) 195–251.
[29] Z. Shao, J. Mou, D.M. Czajkowsky, J. Yang, J.Y. Yuan, Biological atomic force microscopy: what is achieved and what is needed, Adv. Phys. 45 (1996) 1–86.
[30] T.R. Jensen, K. Kjaer, in: D. Mobius, R. Miller (Eds.), Novel Methods to Study Interfacial Layers, Elsevier, New York, 2001, pp. 205–254.
[31] J. Ding, D.Y. Takamoto, A. von Nahmen, M.M. Lipp, K.Y.C. Lee, A.J. Waring, J.A. Zasadzinski, Effects of lung surfactant proteins, SP-B and SP-C, and palmitic acid on monolayer stability, Biophys. J. 80 (2001) 2262–2272.
[32] A. Riechert, H. Ringsdorf, A. Wagenknecht, Spontaneous domain formation of phospholipase A2 at interfaces: fluorescence microscopy of the interaction of phospholipase A2 with mixed monolayers of lecithin, lysolecithin and fatty acid, BBA-Biomembranes 1106 (1992) 178–188.
[33] M.H. Gelb, J.H. Min, M.K. Jain, Do membrane bound enzymes access their substrates from the membrane or aqueous phase: interfacial versus noninterfacial enzymes, BBA-Mol. Cell. Biol. L. 1488 (2000) 20–27.
[34] S. Yapoudjian, M. Ivanova, I. Douchet, A. Zenatti, M. Sentis, W. Marine, A. Svendsen, R. Verger, Surface fluorescence resonance energy transfer studies on interfacial adsorption of thermomyces (Humicola) lanuginosa lipase, using monomolecular films of cis-parinaric acid, Biopolymers 65 (2) (2002) 121–128.
[35] G. Pieroni, Y. Gargouri, L. Sarda, R. Verger, Interactions of lipases with lipid monolayers. Facts and fictions, Adv. Colloid Interface 32 (1990) 341–378.
[36] H.L. Brockman, Kinetic behavior of the pancreatic lipase–colipase–lipid system, Biochimie 82 (2000) 987–995.
[37] T. Tsujita, J.M. Muderhwa, H.L. Brockman, Lipid–lipid interactions as regulators of carboxylester lipase activity, J. Biol. Chem. 264 (1989) 8612–8618.